

Self-Phase Modulation of Silicon Nanostructure Produced By Laser Induced Etching

Hadeel F. Shaker

Bassam G. Rasheed

Laser & Optoelectronic Department, Collage of Engineering, Al-Nahrain University

alqaisi_hadeel@yahoo.com

Abstract

A diode lasers of 532nm and 473nm wavelengths were used to produce silicon nanostructure by laser induced etching process for n-type silicon wafer of orientation <100>. The laser irradiation was carried out using different laser power density of (2, 5, 10 and 20 W/cm² for recorder radiation time (4 min.). Optical fringes due to self-phase modulation are observed. Those fringe patterns depend on the size and depth of the nanostructure. It is found that fast changes in fringes when using short wavelength that indicates to further etching to produced smaller nanostructure at short irradiation time, this procedure could provide valuable details about silicon nanostructure during the etching process (in-situ). Fringes were represented by theoretical model to evaluate the size and change in the refractive index. The AFM images formation of uniform size distribution of 60 nm mean value when laser power density of 20 W/cm² was used for 15 minutes.

Keywords: self –phase modulation, laser induce etching, silicon nanostructure

Introduction

Laser-induced etching process has been used to produce porous silicon consists silicon nanostructure can be defined as a network of nanometer size silicon region surrounded by void space and the size of these voids called pores can vary from few nanometers to few microns. Those structures of various morphologies exhibit significant nonlinear optical properties and open new possibilities for optoelectronics applications [1, 2].

During the photochemical etching process concentric rings of intensity distribution pattern can be observed in the far field of a laser beam. Koker and Kolasinski group have been firstly reported the optical fringe patterns [3]. Series of published papers from this group have observed two clear different sets of fringe patterns: first one includes very small fringe patterns inside the central spot and the other one is the larger outer pattern. They have elucidate the inner fringe patterns by the combined effect of optical interference and Fresnel diffraction of light from

The bottom interface of the film containing nano-Si, but the outer pattern could not be explained by this effect [4 - 6].

The interference patterns can be explained by non-linear phenomenon called self-phase modulation [7]. The change in optical-field-induced refractive index drove to self-induced phase modulation of the beam. The self-phase modulation (SPM) model could be used to estimate the intensity dependence and size dependence change of the refractive index [8].

Analogically, an identical phenomenon of self-phase modulation can occur in space on the transverse intensity profile of a beam, which is known as spatial self-phase modulation, is typical Gaussian profile of the intensity of the laser beam. When an intense laser beam passes through a medium containing nano-Si, the refractive index of the material is altered due to the Gaussian intensity distribution of the laser beam. This change in the refractive index leads to a velocity distribution of the laser beam in the transverse plane. Thus the spatial phase variation occurs in the plane perpendicular to the beam which leads to a visible optical fringe pattern. Those the optical fringe patterns observed in the laser-induced etching arises due to spatial self-phase modulation [9, 10].

The change in refractive index $\Delta n(r)$ for a nonlinear medium is proposed as a function of laser intensity $I(r)$ [11- 13].

$$\Delta n(r) = \gamma_L \cdot I(r) \quad \dots (1)$$

r is a radial distance across the beam.

The nonlinear coefficient γ_L includes the size dependent refractive index and that can defined by equation below

$$\gamma_L = \int_{L_1}^{L_2} f \cdot \frac{N(L)}{L} dL \quad \dots (2)$$

Where f is coupling constant of light with the medium containing Si nanostructure.

$N(L)$ is a Gaussian distribution function for the sizes of nanostructure.

L_1 and L_2 are the minimum and maximum size of the Si nanoparticles used in the Gaussian distribution [3].

A theoretical intensity distribution of the optical Generated fringe pattern is given by the relation [12].

$$I(x) = I_0 \left(\frac{2\pi}{\lambda z} \right)^2 \left| \int_0^\omega \exp \left(-2 \frac{r^2}{\omega^2} - i\Phi(r) \right) r dr J_0 \left(\frac{krx}{2z} \right) \right|^2 \dots (3)$$

Where

$I(x)$ is the far field diffraction of the Gaussian beam.

x is the distance from the center of the far field pattern to the observation point.

$J_0(x)$ the zero order Bessel function of the first kind.

k is the wave number in free space.

Z is the distance from the sample to the observation point.

ω is the waist of laser beam.

$\Phi(r)$ is the phase factor.

The optical fringe patterns could provide important details on the nanostructure sizes and their distribution. Aim of this work is to utilize self-phase modulation occurred in silicon nanostructures to evaluate the size and its distribution during the etching process.

Experimental Procedure

N-type crystalline Silicon wafer of orientation $\langle 100 \rangle$, thickness $500\mu\text{m}$ and resistivity $(10\text{-}30 \Omega\cdot\text{cm})$ samples were cut to pieces dimensions $1 \times 0.5 \text{ cm}$. The wafer was cleaned and immersed in 15% HF diluted with ethanol.

A simple set-up in this work has been used for the LIE process. The set-up consists of a CW diode laser of 532nm wavelength and 50mw power was focused by a focusing lens of 5 cm focal length at the silicon wafer surface. The silicon wafer mounted on two Teflon plates in such a way that the current could pass from the bottom surface to the laser-irradiated area on the top surface through the electrolyte. The electrons are attracted by the holes to the top, therefore, the current pass from bottom to the top and that helps interaction as shown in figure (1) that help the detachment process. Laser beam has a 2.40 eV photon energy calculated from the relation $(E \text{ eV} = \frac{h \cdot c}{\lambda})$ was vertically incident and tilted in a small angle to obtain the interference fringe patterns on a screen as shown in figure (2). The reflected beam from the sample considered as a probe to monitor the etching process. The fringes were recorded by charge-coupled device (CCD) camera and stored in form of a video film. The fringes reported here are the stand-still photographs of the kinetic picture taken by a computer to analyze the optical fringe patterns by image processing program. All freshly prepared samples were stored in a vacuum chamber immediately after preparation.

The surface morphology for both micro and nanostructures of the prepared samples was

investigated by a high resolution optical microscopy, atomic force microscopy (AFM), respectively.

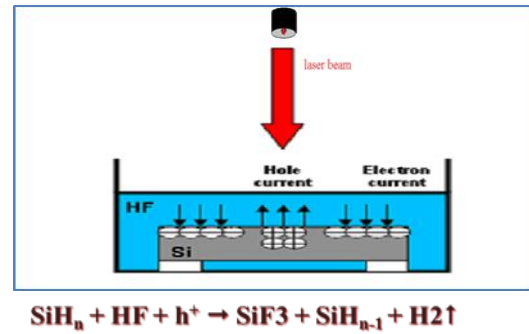


Figure 1: schematic diagram for electron and holes current.

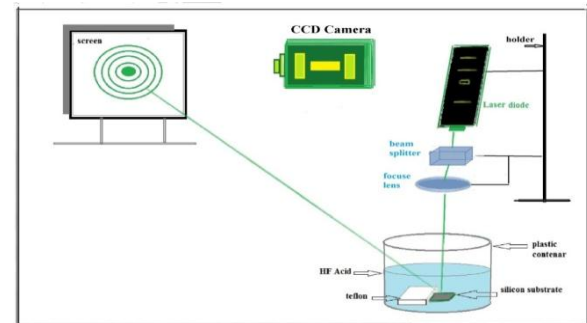


Figure 2: schematic diagram of the experimental setup for laser induced etching process.

Results and Discussion

A. Optical Fringes Pattern

The light reflected from the surface of the sample manifests itself into a concentric multiple diffraction patterns for the nan crystals can be observed on the screen. This indicate that quantum confinement effect augment swiftly the nonlinearity of the refractive index. However, it is observed that the evolution of the optical fringe pattern depends upon the fabrication parameters such as the irradiation time, probing laser power densities, wavelength of the laser, resistivity of crystalline silicon and the hydrofluoric acid concentration. The experimental results from observed fringe patterns have been used to calculate various theoretical parameters such as mean value of silicon nan crystallites sizes (L_0) and their distribution (L_1 & L_2) and optical parameters using the nonlinear equations that mentioned in section of introduction, **Mathcad 7 professional software package** is used to calculate the theoretical parameters and clearly plotted the fringes number, also it is used to find out the magnitude of nonlinear refractive index variation of nano- Si using equation (1).

The time evolution of the far field optical fringe patterns from a sample etched by different laser power density (2, 5, 10, and 20 W/cm^2) of

irradiation time 5 min has been studied. The theoretical plot of this relation is in pact with the optical fringes that experimentally observed during laser induced etching of silicon. Figure (3)

(a, b, c, d) shows the photographs of the optical fringes for probing laser power densities (2, 5, 10, 20 W/cm^2) respectively

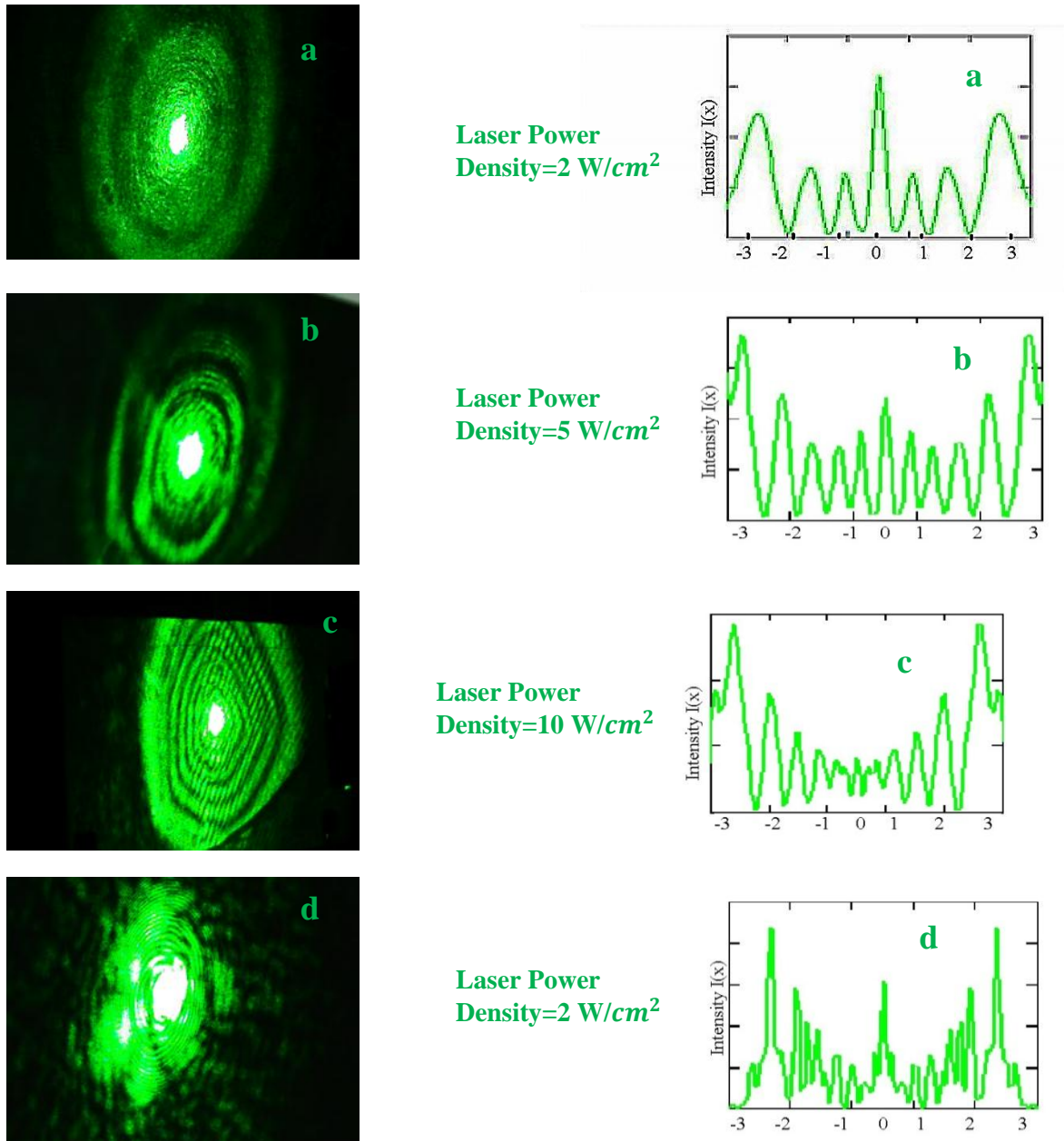


Figure 3: The experimentally observed optical fringe patterns with their corresponding theoretical representation from nano-silicon prepared at irradiation time 4 minute with 532nm laser wavelength

It is observed that the numbers of optical fringe patterns including the central spot are increases withincreasing laser power density and the fringes spacing become narrower when the power density increases. This could be attributed to the subsequent changes of the refractive index of the medium constituting silicon nanostructures and consequently changes the fringe patterns. The corresponding theoretical results for those optical fringe patterns reliable as far as the number of

fringes and the equidistant fringe spacing are concerned. Although a part of the laser beam reflecting from the HF surface and from the top of the surface of the silicon substrate are expected to be very bright. Fitting the experimentally observed fringe patterns with theoretical model of the self-phase modulation provide valuable details concerning the etching formation mechanism, silicon Nano crystallite and their size distribution. Table (1)

gives values of mean size for silicon nanocrystallites (L_0) and their distributions (L_1 & L_2). Increasing the laser power density leads to increase silicon nanocrystallites where smaller sizes are obtained for lower laser power density, that are due to the slow chemical reaction between silicon wafer and HF acid, whereas, low laser power density supplies low holes generation and subsequent slow chemical reaction. That also mean high laser power density lead to fast etching rate (speed process) so the surface supposed to be polished revealing the new porous layer small thickness. Moreover, table (2) gives values for comparison between blue and green laser wavelength. These values reveal formation of smaller nanostructures at short wavelength with short irradiation time.

Table 1: represents the nanocrystallite sizes for different probing laser power density and the experimentally measurements

Power density (W/cm^2)	L1(nm)	L0(nm)	L2(nm)
2	1.7	2.2	5.6
5	1.8	2.4	5.9
10	0.9	2.6	5.6
20	1.2	2.7	4.9

Table 2: represent the mean nanocrystal size, number of fringes patterns and change in refractive Index for blue and green diode lasers at 4 min.

Wavelength (nm)	Lo (nm)	No. of fringes	Δn
473	3	7	0.22
532	4.8	4	0.27

Figure (4) represents effect of laser power density on mean value of silicon nanocrystallites. Moreover, one can clearly observe that number of fringes patterns increase with laser power density as shown in figure (5 a). This is attributed of the formation of large number of silicon nanocrystallites. Porous silicon consist silicon nanostructure product by LIE process have advantage of its unique optoelectronic properties, furthermore increase in refractive index make nano-silicon posse's physical characteristics can be very different from those of bulk counterparts, which can be used in many applications, therefore from our calculations reveal that change in refractive index was optimum at ($10 W/cm^2$) can show in figure (5 b), this optimum value depends on the employed laser wavelength and it is found at ($8 W/cm^2$) for the blue laser wavelength (473 nm)

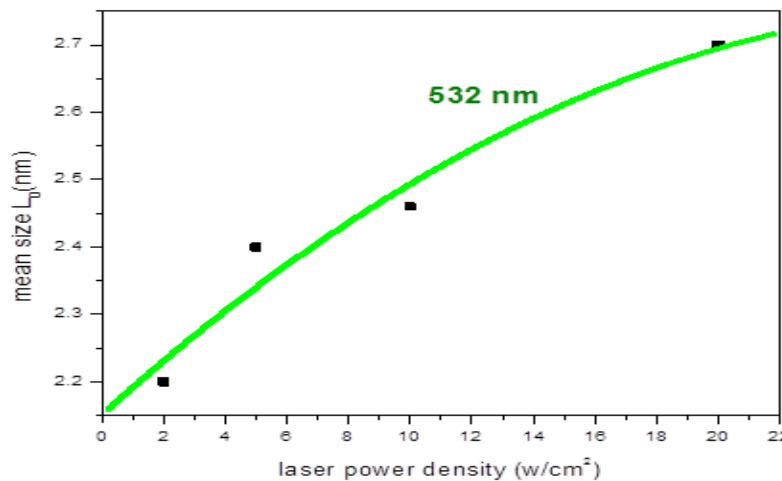


Figure 4: the relation between laser power density and mean nanocrystallites size.

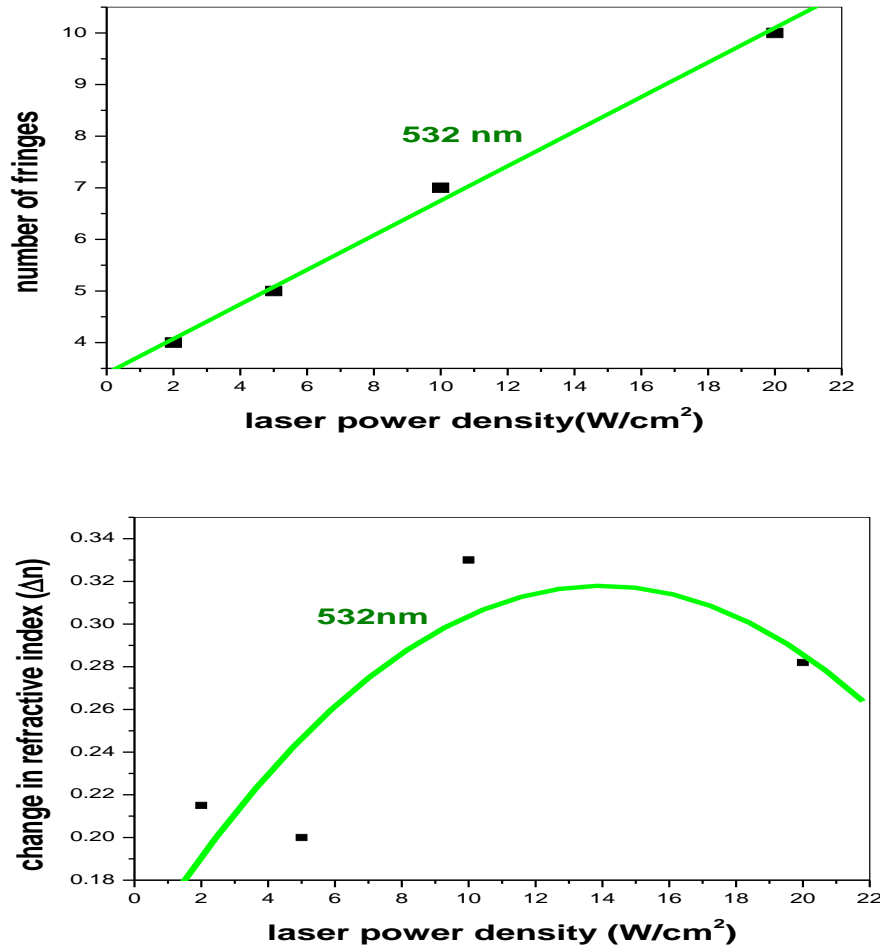


Figure 5: the relationship of laser power density with (a) number of fringes (b) Change in refractive index.

B. Surface morphology

One of the most powerful characterization techniques is the surface morphology. Two morphological instruments were employed (the atomic force microscope AFM to examine the top surface of silicon nanostructure and high resolution optical microscope to investigate the microstructure of the same sample). Figure (6) shows images from high resolution optical microscopy to investigate the microstructure of the same sample and to measure the thickness (depth) microstructure of the P-Si layer by image analysis. Surface plots were used another software program (**image J**). The experimentally prepared sample for irradiation time 5min, HF acid concentration 15%, laser wavelength 532nm for different laser power density. For P.D of 5 W/cm², few numbers of very small pores and irregular shape of pores were observed.

At lower laser power densities, small numbers of electron-hole pairs are generated, therefore, weak chemical reaction initiated at the Si wafer surface which leads to form small porous layer thickness. Then large numbers of e-h pairs are

generated at higher laser power densities and density of nanostructures are observed in figure (6 a). It seems that the pore formation commenced with the initiation of the etching process on the silicon surface. On increasing P.D to 10 W/cm², a larger number of pores containing silicon nanostructures appear on the surface, can clearly observe that in figure (6 b). These pores distributed within a distance close the penetration depth of the laser wavelength. The nanostructures of relatively large size are distributed on the etched area when the laser power density increases to 20 W/cm². On increasing power density to 20 W/cm², more holes reach the surface leading to further dissolving of the Si and excessive etching as shown in figure (6 c), from this figure observed different color on surface of porous layer that because the morphology of thickness of Porous layer and the different in the structure sizes and shapes formed on the surface at this P.D of laser.

Furthermore, some fine features could also be seen using AFM. The detailed observation of

smaller nanostructure is made difficult due to the rough surface morphology on the top nanostructured surface. The samples etched by laser demonstrate by AFM images. Figure (7) illustrates a wide non homogeneous with average size of 80 nm when 5 W/cm^2 laser power density was used, While homogeneous silicon nanocrystallites size distribution around 60 nm average size for 10 W/cm^2 . That is due to e-h pairs generation and their effect since the required holes can be generated by higher laser power

density. The surface roughness and the variation in nanoscale features developed over the Si surface due to laser power density. As the power density is increased from $10\text{ to }20\text{ W/cm}^2$, more Silicon nanostructures of a sharper shape were distinguished. The size, depth and shape of nanocrystallites Si are dependent on the laser power density and the irradiation time. Therefore, the specifications of the porous layer and its applications can be determined by those effective parameters.

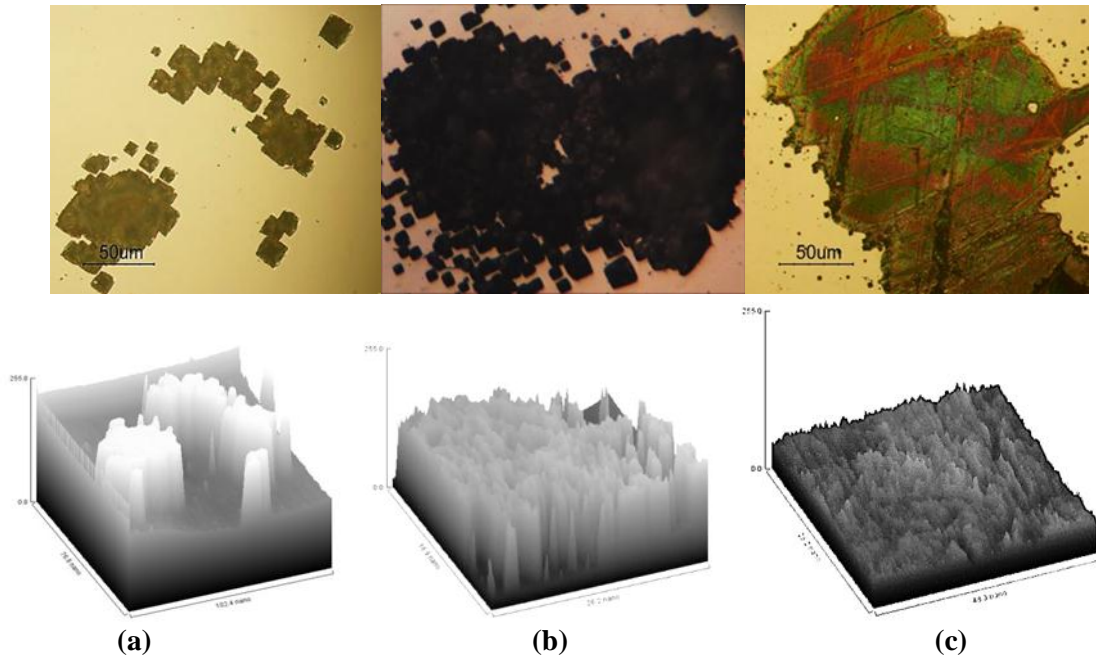


Figure 6: the optical microscope images with corresponding surface plot of nanostructure for different laser power (a,b,c) for 5 W/cm^2 , 10 W/cm^2 and 20 W/cm^2 respectively .

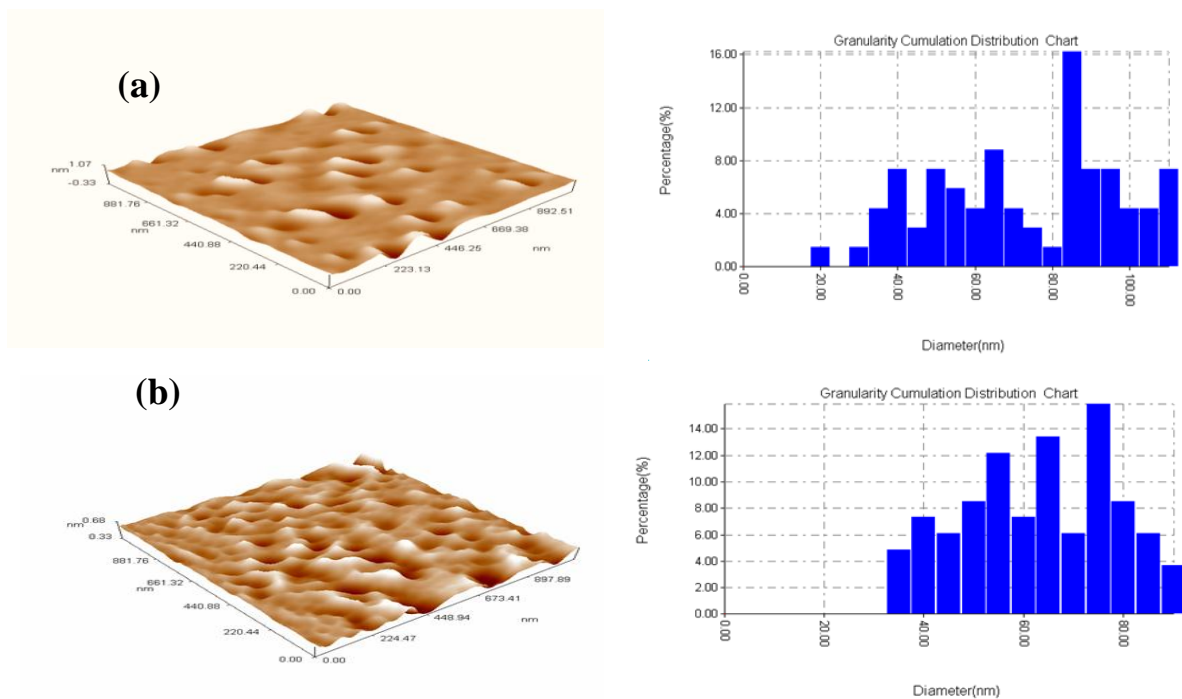


Figure 7: Atomic force microscope images for silicon substrate of orientation $\langle 100 \rangle$, for wavelength 532 nm and irradiation time 15 min . (a) 10 W/cm^2 and (b) 20 W/cm^2 .

Conclusion

The laser beam produces non-linear phenomenon called self-phase modulation when propagates in silicon nanostructure. The nonlinear change of refractive index of the silicon nanostructures depends on the laser power and size of nano-silicon that are calculated by self-phase modulation model. The magnitude of the nonlinear refractive index was changed with the probe laser power density. Smaller silicon nanocrystallite sizes could be achieved using lower power density with suitable effective parameters like etching time and solution concentration of HF. The numbers of optical fringe patterns including the central spot are increases with the probing laser power density increases. Theoretical model based on self-phase modulation can be adopted to evaluate size, size distribution and change in refractive index. Work utilizes blue laser wavelength to produce silicon nanostructure and compared with those of green laser.

References

- [1] H.S. Mavi, B.G. Rasheed, A.K. Shukla, S.C. Abbi and K.P. Jain, “**Spectroscopic investigations of porous silicon prepared by laser-induced Etching of silicon**”, Journal of Physics D: Applied Physics, vol. 34, no.3 (2001).
- [2] L. Pavesi and R. Turan, “**Silicon Nanocrystals Fundamentals, Synthesis and Applications**”, WILEY-VCH Verlag GmbH & Co. KGaA, Weinheim (2010).
- [3] [3] B. G. Rasheed, S. Mavi, A. K. Shukla, S. C. Abbi and K. P. Jain, “**Surface reconstruction of silicon and polysilicon by Nd: YAG laser etching: SEM, Raman and PL studies**” Mate. Sci. and Eng. B 79 pp. 71-77(2001).
- [4] L. Koker and K.W. Kolasinski, “**observation and application of optical interference and diffraction effects in reflection from photochemically fabricated Gaussian interfaces**”, J. Appl. Phys. 86 no.4, pp.1800-1807 (1999).
- [5] K.W. Kolasinski, J.C. Bernard, L. Koker, S. Ganguly and R.E. Palmer, “**in situ photoluminescence studies of photochemically grown porous silicon**” Mat. Sci. & Eng. B. 69 ,157-160 (2000) .
- [6] L. Koker, K.W. Kolasinski, “**applications of a novel method for determining the rate of production of photochemical porous silicon**” Mat. Sci. & Eng. B, 69-70 (2000) 132-135.
- [7] Y.R. Shen, “**The Principles of Nonlinear Optics**”, (John Wiley & Sons, New York, 303, (1984).
- [8] H.S. Mavi, S. Prusty, A.K. Shukla and S.C. Abbi, “**Nonlinear phenomenon in nanocrystallites produced by laser-induced etching of silicon**” opt. Commun. 226, pp 405-413, (2003) .
- [9] S.D. Durbin, S.M. Arakelian and Y.R. Shen, “**Laser- induced diffraction rings from a nematic liquid-crystal film**”, Optics Letters, vol. 6, no. 9, pp. 411-413 (1981).
- [10] K. A. Nawakoski, “**laser beam interaction with material for microscale applications**”, nanoengineering, science, and technology (2005).
- [11] S. Prusty, H.S. Mavi and A.K. Shukla, “**Optical nonlinearity in silicon nanoparticles: Effect of size and probing intensity**” Phys. Rev B 71, 113313(2005).
- [12] H.Ono and Y. Harato “**characterization of laser- induced self-phase modulation in host-guest liquid crystals**”, japan .J.Appl.Phys.Vol. 37, (1998).
- [13] Tayyar Dzhafarov, “**Silicon Solar Cells with Nanoporous Silicon Layer** “ solar cells – Research and Application Perspectives , Edited by Arturo Morales-Acevedo, InTech, (2013).

تضمين الطور الذاتي لتراكيب السليكون النانوية المنتجة بالليزر

بسام غالب رشيد

هديل فائز شاكر

قسم هندسة الليزر والالكترونيات البصرية، كلية الهندسة، جامعة النهريين

الخلاصة:

تم تحضير سطح سليكوني مسامي ذو تراكيب نانوية فوق شريحة السليكون يمتاز هذا السطح بخصائص متنوعة من خلال عملية التتميش الضوئي باستخدام ليزرات بأطوال موجي 532 نانومتر و473 نانومتر لتشجيع شريحة السليكون من نوع (n-type) وبإتجاهية <100>. تم دراسة تأثير كثافة قدرة الليزر على خصائص طبقة السليكون النانوية باستخدام كثافة طاقة مختلفة وهي (2، 5، 10، 20 واط/سم²) بزمن تشعيع قياسي اربع دقائق، ووجد بأن طبقة التركيب النانوي تولد نموذج الأهداب البصرية بسبب تأثير الحصر الكمي وتتغير هذه الأهداب بالاعتماد على عمق الحفر واحجام التراكيب النانوية المتكونة على السطح ووجد بان التغير السريع بالأهداب عند استخدام طول موجي قصير هو نتيجة سرعة عملية التتميش وتكوين تراكيب متناهية الصغر وان هذه التقنية ممكن الحصول على تفاصيل وقيم للتراكيب النانوية المتكونة اثناء عملية التتميش. وقد أستُخدم النموذج الرياضي بالاعتماد على تضمين الطور الذاتي لدراسة تأثير كثافة قدرة الليزر على الأهداب البصرية ومقدار التغير في معامل الإنكسار وحساب قيم تقديرية لحجم تراكيب السليكون النانوية وتوزيعها على السطح. أجريت دراسة على طوبوغرافية السطح باستخدام مجهر القوى الذرية، وتم الحصول على أحجام لتراكيب السليكون النانوية بمعدل 60 نانومتر متوزعة بشكل منتظم على سطح السليكون عند استخدام كثافة طاقة 20 واط/سم² بزمن تشعيع 15 دقيقة.